

# **LABORATORY EXPERIMENT 2:**

## **FRACTURE CHARPY TESTING REPORT**

**Henri Tuoma 549707**

**Jonathan Lundström, 708593**

**Markus Forsback 493905**

**Binh Nguyen 887799**

**Topi Laitinen 100603611**

<b>1. Introduction</b>	<b>4</b>
<b>2. Methods</b>	<b>5</b>
2.1 Testing samples	5
2.2 Testing environment	5
2.3 Test equipment	6
<b>3. Results</b>	<b>12</b>
3.1 Mandatory information	12
3.1.a Reference report	12
3.1.b Identification of the test piece (e.g. type of steel and cast number)	12
3.1.c Size of the test piece, if other than the standard test piece	12
3.1.d Temperature of the test specimens (Table 2)	13
3.1.e Absorbed energy	13
3.1.f Whether the specimen, or the majority of specimens in a group of specimens were broken	
13	
3.1.g Any abnormalities that could have affected the test	13
3.2 Optional information	14
3.2.a Test piece orientation (ISO 3785)	14
3.2.b Initial potential energy of the testing machine, in joules	15
3.2.c Lateral expansion (Annex B)	16
3.2.d Shear fracture appearance (see Annex C)	17
3.2.e Absorbed energy/temperature curve (Annex D.1)	18
3.2.f Lateral expansion/temperature curve	20
3.2.g Shear fracture appearance/temperature curve	21
3.2.h Transition temperatures and determination criteria (Annex D.2)	23
3.2.i Number of test pieces which were not completely broken in the test	27
3.2.j Date of the most recent full direct and indirect verifications	27
3.2.k Measurement uncertainty of the absorbed energy (Annex E)	28
<b>4. Discussion</b>	<b>28</b>
4.1 Result analysis	28
4.2 Differences in fracture behavior in various temperatures	29
4.3 Reliability of results	29
4.4 Brief conclusion	30
<b>References</b>	<b>30</b>

## Symbols

Table 1. Symbols

<b>Symbol</b>	<b>Unit</b>	<b>Designation</b>
B	(mm)	Thickness of the specimen
L	(mm)	Length of the specimen
K	J	Absorbed energy
KV2	J	Absorbed energy for a V-notch test piece using 2mm striker
KV8	J	Absorbed energy for a V-notch test piece using 8mm striker
KU2	J	Absorbed energy for a U-notch test piece using 2mm striker
KU8	J	Absorbed energy for a U-notch test piece using 8mm striker
T	°C	Temperature
Tt	°C	Transition temperature
LE	mm	Lateral expansion
Kn	J	Nominal initial potential energy
P	%	Percentage of ductile fracture
Kp	J	Initial potential energy

# 1. Introduction

Whether a material is used in an everyday product or a critical structure, it is subject to different mechanical stresses and environmental conditions. It is important to know the materials' properties while choosing a material for a specific part. One fundamental aspect of materials behavior that can have an impact on their performance is the way they fracture when subjected to external forces. Material fractures can be brittle, ductile, or mixed mode. The degree of ductile fracture depends on the material's temperature. Knowing this behavior of the materials, we can choose one that is not brittle in the product's operating temperature, avoiding fatal breakdowns due to brittle fracture.

The material's toughness in different temperatures is an important property when choosing a material. With the Charpy pendulum impact test according to the standard ISO 148-1:2015, we could determine a material's impact toughness at specific temperatures (SUOMEN STANDARDISOIMISLIITTO SFS, 2016). In the test, samples of specified dimensions are broken into 2 pieces by a swinging pendulum. This pendulum is hung on the air with a known initial potential energy. After that, it is released and breaks the sample, where the necessary potential energy to break it can be measured. The impact toughness is a measure of the energy absorbed by the material before and during fracture, a brittle material absorbs a lower energy than a ductile material (Hertzberg, 2012, 266-269). Also, the fracture surface is inspected for plastic deformation to determine if it is brittle or ductile fracture.

Body-centered cubic (BCC) metals are more sensitive than face-centered cubic (FCC) metals with the temperature sensitivity of the fracture mechanism. That is due to the larger temperature sensitive Peierls-Nabarro stress contribution in BCC metals than in FCC metals (Hertzberg, 2012, 307). The Peierls-Nabarro stress resists lattice movement, which is also plastic deformation, because of this the materials become brittle at lower temperature (Hertzberg, 2012, 70-71). The behavior is seen in ceramics and metals, which are more sensitive to temperature than those with narrow lattice structures (Hertzberg, 2012, 71).

Gaining data from a Charpy pendulum test includes multiple sources of uncertainties. These different uncertainties such as material inhomogeneity, temperature bias and machine bias can be calculated and reported with the test results according to the ISO 148-1:2015 (SUOMEN STANDARDISOIMISLIITTO SFS, 2016). The more samples tested, the more accurate data is gained from the tests. However, for quality check, this test is a relatively simple fail or pass test.

This report includes the methods used for executing a Charpy pendulum test according to the ISO 148-1:2015 standard at a specified temperature. The results presented are from the testing as well as from tests completed by other laboratory groups. Finally, the results are discussed and the reliability of the results are evaluated.

## 2. Methods

### 2.1 Testing samples

Testing samples were prepared following SFS-EN ISO 148-1. The sample preparation was done prior to the lab session, and was not completely according to the standard. Instead of machining the samples from a larger piece, the samples were cut from an off-the-shelf steel bar with 10 by 10 mm cross section, and V-notches were machined to them according to the dimensions specified in ISO 148-1. Therefore, the outside dimensions of the test pieces do not adhere to the dimensional tolerances specified in the standard.

### 2.2 Testing environment



Figure 1. In the upper box, a mixture of liquid nitrogen and ethanol (-30 celsius) was included, and in the lower box, pure liquid nitrogen (-196 celsius) was included.

In the experiment, we have three environments for three different temperatures:

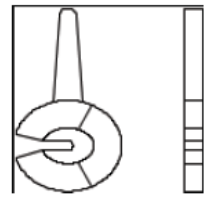
1. Room temperature, which was measured to be 19,5 celsius.
2. The box below, which contains liquid hydrogen at an extremely cold temperature of -196 C. One sample is conditioned to approximately -60 celsius in this container to demonstrate clearly brittle fracture behavior
3. The box above, which contains liquid hydrogen mixed with ethanol to maintain the temperature at -30 Celsius. There are four samples tested in this temperature.

## 2.3 Test equipment

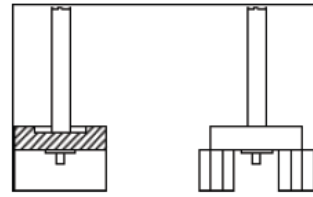


*Figure 2. Charpy pendulum impact testing machine.*

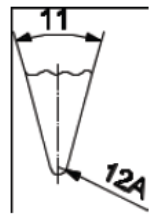
The Charpy pendulum impact testing machine consists of the hammer, striker parts and an anvil, which is a support for the Charpy test specimen. The test is performed by the hammer swinging from a fixed location at the top side of the pendulum. The fixed location can be seen in figure 7. After swinging down, the striker part, which is installed on the hammer, strikes the Charpy test specimen that rests on the anvil at the bottom of the pendulum's path. The Charpy test specimen is prepared by having a small notch which helps the material to break, in this case a V-notch. If everything goes according to plan, the striker part inflicts high concentration of force into the Charpy test specimen and it breaks. The striker used in this pendulum impact testing machine was a 2mm striker and the hammer was a C-type hammer. In figure 3, we can see the specifics of the types more closely.



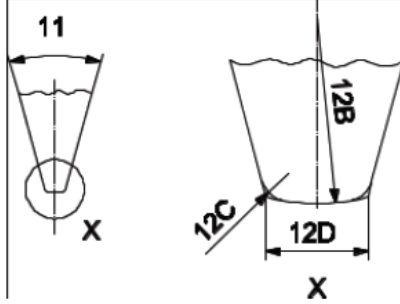
a) C-type hammer



b) U-type hammer



c) 2 mm striker



d) 8 mm striker

Figure 3. Different types for hammer and striker parts. The hammer type we had in the experiment was a) C-type hammer and the striker was c) 2mm striker. Figure adapted from SFS-EN ISO 148-2.

## 2.4 Testing procedure

### 2.4.1. Measurement of the test pieces

Before the test, the measurements of the test sample dimensions were taken with a vernier caliper. The results are shown in Table 2. Measured values were the width and thickness of the test samples. The width means the distance between the notched face and its opposite face (ISO148). The thickness means the dimension, which is perpendicular to the width and parallel to the notch (ISO 148). The test samples were numbered, so that identification of the sample is easier during the test. After measurement, the values were written down to the sheet given by the laboratory.



Figure 4. Test samples before the test, numbered in the ends of the samples.

### 2.4.2 Friction measurement

According to ISO 148, the energy absorbed by friction (air resistance, bearing friction, friction of the indicating pointer) shall be measured prior to the test and also other methods can be applied than the standard's procedure. In this test, it was checked before the tests, how much energy the pendulum swing absorbs without a test sample in the machine. The value for this was 4 joules. This value has not been subtracted from the test results, because the linearity of the energy loss during the pendulum swing is not known. Therefore, this hasn't been subtracted from the value of energy loss during the impact.

### 2.4.3. Cooling the samples

Before the impact test, the testing samples were conditioned either in a mixture of liquid nitrogen and ethanol, or pure liquid nitrogen. The samples conditioned in the ethanol-LN mixture were kept there for at least 5 minutes in order for the temperature to stabilize all throughout the samples. The one sample conditioned in pure liquid nitrogen was cooled for a couple of minutes and removed from the container while the nitrogen was still boiling. Therefore, the sample had not reached the temperature of the liquid nitrogen, but an experienced laboratory technician estimated that it was approximately -60 celsius.



Figure 5. Box of cooling agent and thermometer measuring the sample's temperature.

### 2.4.4. Sample transfer to Charpy impact testing machine.

After the sample had been in the cooling agent for the measured time, it was transferred to the testing machine using modified pliers for that use. In the pliers, there was a block attached to the tip, towards which the test sample can be pressed. In the impact testing machine, there was a slot with the same length as the block in the plier's tip. The block was fitted to the slot, which helped to set the test sample in the right position to the test machine. This can be one reason for variation in results, if the position of the test sample changes compared to the block in the tool.

In ISO 148, the transfer time of the samples from the heating or cooling to the testing machine shall be no more than 5 seconds, if the temperature between ambient or instrument temperature and the test sample is not under 25 celsius. If the difference is under 25 celsius, the time shall be no more than 10 seconds.



Figure 6. The tool used to transfer the test sample with the block attached to the tip.

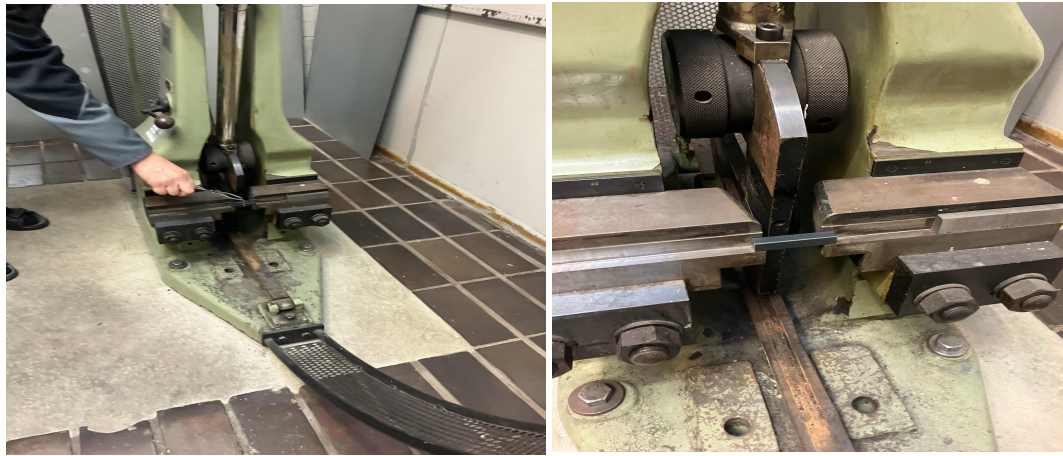


*Figure 7. Setting the test sample to the Charpy impact test machine.*

#### **2.4.5. Lifting the pendulum up for the test**

To conduct the impact test, the pendulum needs to be lifted and locked to the up position first by swinging it slightly to lift it more easily. After locking the pendulum to the up position, the lock could be released and the pendulum could break the test sample.



*Figure 8. Releasing the pendulum from the up position.*

## 2.4.6. Reading the results

After conducting the test, absorbed energy value can be read from the Charpy-machine's measurement scale as demonstrated in Figure 8. From the measurement-scale, the middle scale was used to find out the amount of absorbed energy by the test sample. Furthermore, dimensions of the test pieces were measured with Vernier caliper to define lateral expansion, and the fracture surfaces were examined visually to assess the percentages of ductile and shear fracture.



Figure 8. Charpy-machine indicating the absorbed energy value after the test has been conducted.

## 2.4.7. Documenting the results

Finally the results were collected to a sheet which was provided by the laboratory, which included test sample temperature, impact energy, whether it was broken in half, width, thickness before and after test, and percentage of ductile fracture.

TEST NO.	TEST DATE	TESTER	TESTER SIGNATURE	TESTER NUMBER
1	1/2/16	1/2/16	1/2/16	1/2/16
2	1/2/16	1/2/16	1/2/16	1/2/16
3	1/2/16	1/2/16	1/2/16	1/2/16
4	1/2/16	1/2/16	1/2/16	1/2/16
5	1/2/16	1/2/16	1/2/16	1/2/16
6	1/2/16	1/2/16	1/2/16	1/2/16
7	1/2/16	1/2/16	1/2/16	1/2/16
8	1/2/16	1/2/16	1/2/16	1/2/16
9	1/2/16	1/2/16	1/2/16	1/2/16
10	1/2/16	1/2/16	1/2/16	1/2/16
11	1/2/16	1/2/16	1/2/16	1/2/16
12	1/2/16	1/2/16	1/2/16	1/2/16
13	1/2/16	1/2/16	1/2/16	1/2/16
14	1/2/16	1/2/16	1/2/16	1/2/16
15	1/2/16	1/2/16	1/2/16	1/2/16
16	1/2/16	1/2/16	1/2/16	1/2/16
17	1/2/16	1/2/16	1/2/16	1/2/16
18	1/2/16	1/2/16	1/2/16	1/2/16
19	1/2/16	1/2/16	1/2/16	1/2/16
20	1/2/16	1/2/16	1/2/16	1/2/16
21	1/2/16	1/2/16	1/2/16	1/2/16
22	1/2/16	1/2/16	1/2/16	1/2/16
23	1/2/16	1/2/16	1/2/16	1/2/16
24	1/2/16	1/2/16	1/2/16	1/2/16
25	1/2/16	1/2/16	1/2/16	1/2/16
26	1/2/16	1/2/16	1/2/16	1/2/16
27	1/2/16	1/2/16	1/2/16	1/2/16
28	1/2/16	1/2/16	1/2/16	1/2/16
29	1/2/16	1/2/16	1/2/16	1/2/16
30	1/2/16	1/2/16	1/2/16	1/2/16
31	1/2/16	1/2/16	1/2/16	1/2/16
32	1/2/16	1/2/16	1/2/16	1/2/16
33	1/2/16	1/2/16	1/2/16	1/2/16
34	1/2/16	1/2/16	1/2/16	1/2/16
35	1/2/16	1/2/16	1/2/16	1/2/16
36	1/2/16	1/2/16	1/2/16	1/2/16
37	1/2/16	1/2/16	1/2/16	1/2/16
38	1/2/16	1/2/16	1/2/16	1/2/16
39	1/2/16	1/2/16	1/2/16	1/2/16
40	1/2/16	1/2/16	1/2/16	1/2/16
41	1/2/16	1/2/16	1/2/16	1/2/16
42	1/2/16	1/2/16	1/2/16	1/2/16
43	1/2/16	1/2/16	1/2/16	1/2/16
44	1/2/16	1/2/16	1/2/16	1/2/16
45	1/2/16	1/2/16	1/2/16	1/2/16
46	1/2/16	1/2/16	1/2/16	1/2/16
47	1/2/16	1/2/16	1/2/16	1/2/16
48	1/2/16	1/2/16	1/2/16	1/2/16
49	1/2/16	1/2/16	1/2/16	1/2/16
50	1/2/16	1/2/16	1/2/16	1/2/16
51	1/2/16	1/2/16	1/2/16	1/2/16
52	1/2/16	1/2/16	1/2/16	1/2/16
53	1/2/16	1/2/16	1/2/16	1/2/16
54	1/2/16	1/2/16	1/2/16	1/2/16
55	1/2/16	1/2/16	1/2/16	1/2/16
56	1/2/16	1/2/16	1/2/16	1/2/16
57	1/2/16	1/2/16	1/2/16	1/2/16
58	1/2/16	1/2/16	1/2/16	1/2/16
59	1/2/16	1/2/16	1/2/16	1/2/16
60	1/2/16	1/2/16	1/2/16	1/2/16
61	1/2/16	1/2/16	1/2/16	1/2/16
62	1/2/16	1/2/16	1/2/16	1/2/16
63	1/2/16	1/2/16	1/2/16	1/2/16
64	1/2/16	1/2/16	1/2/16	1/2/16
65	1/2/16	1/2/16	1/2/16	1/2/16
66	1/2/16	1/2/16	1/2/16	1/2/16
67	1/2/16	1/2/16	1/2/16	1/2/16
68	1/2/16	1/2/16	1/2/16	1/2/16
69	1/2/16	1/2/16	1/2/16	1/2/16
70	1/2/16	1/2/16	1/2/16	1/2/16
71	1/2/16	1/2/16	1/2/16	1/2/16
72	1/2/16	1/2/16	1/2/16	1/2/16
73	1/2/16	1/2/16	1/2/16	1/2/16
74	1/2/16	1/2/16	1/2/16	1/2/16
75	1/2/16	1/2/16	1/2/16	1/2/16
76	1/2/16	1/2/16	1/2/16	1/2/16
77	1/2/16	1/2/16	1/2/16	1/2/16
78	1/2/16	1/2/16	1/2/16	1/2/16
79	1/2/16	1/2/16	1/2/16	1/2/16
80	1/2/16	1/2/16	1/2/16	1/2/16
81	1/2/16	1/2/16	1/2/16	1/2/16
82	1/2/16	1/2/16	1/2/16	1/2/16
83	1/2/16	1/2/16	1/2/16	1/2/16
84	1/2/16	1/2/16	1/2/16	1/2/16
85	1/2/16	1/2/16	1/2/16	1/2/16
86	1/2/16	1/2/16	1/2/16	1/2/16
87	1/2/16	1/2/16	1/2/16	1/2/16
88	1/2/16	1/2/16	1/2/16	1/2/16
89	1/2/16	1/2/16	1/2/16	1/2/16
90	1/2/16	1/2/16	1/2/16	1/2/16
91	1/2/16	1/2/16	1/2/16	1/2/16
92	1/2/16	1/2/16	1/2/16	1/2/16
93	1/2/16	1/2/16	1/2/16	1/2/16
94	1/2/16	1/2/16	1/2/16	1/2/16
95	1/2/16	1/2/16	1/2/16	1/2/16
96	1/2/16	1/2/16	1/2/16	1/2/16
97	1/2/16	1/2/16	1/2/16	1/2/16
98	1/2/16	1/2/16	1/2/16	1/2/16
99	1/2/16	1/2/16	1/2/16	1/2/16
100	1/2/16	1/2/16	1/2/16	1/2/16
101	1/2/16	1/2/16	1/2/16	1/2/16
102	1/2/16	1/2/16	1/2/16	1/2/16
103	1/2/16	1/2/16	1/2/16	1/2/16
104	1/2/16	1/2/16	1/2/16	1/2/16
105	1/2/16	1/2/16	1/2/16	1/2/16
106	1/2/16	1/2/16	1/2/16	1/2/16
107	1/2/16	1/2/16	1/2/16	1/2/16
108	1/2/16	1/2/16	1/2/16	1/2/16
109	1/2/16	1/2/16	1/2/16	1/2/16
110	1/2/16	1/2/16	1/2/16	1/2/16
111	1/2/16	1/2/16	1/2/16	1/2/16
112	1/2/16	1/2/16	1/2/16	1/2/16
113	1/2/16	1/2/16	1/2/16	1/2/16
114	1/2/16	1/2/16	1/2/16	1/2/16
115	1/2/16	1/2/16	1/2/16	1/2/16
116	1/2/16	1/2/16	1/2/16	1/2/16
117	1/2/16	1/2/16	1/2/16	1/2/16
118	1/2/16	1/2/16	1/2/16	1/2/16
119	1/2/16	1/2/16	1/2/16	1/2/16
120	1/2/16	1/2/16	1/2/16	1/2/16
121	1/2/16	1/2/16	1/2/16	1/2/16
122	1/2/16	1/2/16	1/2/16	1/2/16
123	1/2/16	1/2/16	1/2/16	1/2/16
124	1/2/16	1/2/16	1/2/16	1/2/16
125	1/2/16	1/2/16	1/2/16	1/2/16
126	1/2/16	1/2/16	1/2/16	1/2/16
127	1/2/16	1/2/16	1/2/16	1/2/16
128	1/2/16	1/2/16	1/2/16	1/2/16
129	1/2/16	1/2/16	1/2/16	1/2/16
130	1/2/16	1/2/16	1/2/16	1/2/16
131	1/2/16	1/2/16	1/2/16	1/2/16
132	1/2/16	1/2/16	1/2/16	1/2/16
133	1/2/16	1/2/16	1/2/16	1/2/16
134	1/2/16	1/2/16	1/2/16	1/2/16
135	1/2/16	1/2/16	1/2/16	1/2/16
136	1/2/16	1/2/16	1/2/16	1/2/16
137	1/2/16	1/2/16	1/2/16	1/2/16
138	1/2/16	1/2/16	1/2/16	1/2/16
139	1/2/16	1/2/16	1/2/16	1/2/16
140	1/2/16	1/2/16	1/2/16	1/2/16
141	1/2/16	1/2/16	1/2/16	1/2/16
142	1/2/16	1/2/16	1/2/16	1/2/16
143	1/2/16	1/2/16	1/2/16	1/2/16
144	1/2/16	1/2/16	1/2/16	1/2/16
145	1/2/16	1/2/16	1/2/16	1/2/16
146	1/2/16	1/2/16	1/2/16	1/2/16
147	1/2/16	1/2/16	1/2/16	1/2/16
148	1/2/16	1/2/16	1/2/16	1/2/16
149	1/2/16	1/2/16	1/2/16	1/2/16
150	1/2/16	1/2/16	1/2/16	1/2/16
151	1/2/16	1/2/16	1/2/16	1/2/16
152	1/2/16	1/2/16	1/2/16	1/2/16
153	1/2/16	1/2/16	1/2/16	1/2/16
154	1/2/16	1/2/16	1/2/16	1/2/16
155	1/2/16	1/2/16	1/2/16	1/2/16
156	1/2/16	1/2/16	1/2/16	1/2/16
157	1/2/16	1/2/16	1/2/16	1/2/16
158	1/2/16	1/2/16	1/2/16	1/2/16
159	1/2/16	1/2/16	1/2/16	1/2/16
160	1/2/16	1/2/16	1/2/16	1/2/16
161	1/2/16	1/2/16	1/2/16	1/2/16
162	1/2/16	1/2/16	1/2/16	1/2/16
163	1/2/16	1/2/16	1/2/16	1/2/16
164	1/2/16	1/2/16	1/2/16	1/2/16
165	1/2/16	1/2/16	1/2/16	1/2/16
166	1/2/16	1/2/16	1/2/16	1/2/16
167	1/2/16	1/2/16	1/2/16	1/2/16
168	1/2/16	1/2/16	1/2/16	1/2/16
169	1/2/16	1/2/16	1/2/16	1/2/16
170	1/2/16	1/2/16	1/2/16	1/2/16
171	1/2/16	1/2/16	1/2/16	1/2/16
172	1/2/16	1/2/16	1/2/16	1/2/16
173	1/2/16	1/2/16	1/2/16	1/2/16
174	1/2/16	1/2/16	1/2/16	1/2/16
175	1/2/16	1/2/16	1/2/16	1/2/16
176	1/2/16	1/2/16	1/2/16	1/2/16
177	1/2/16	1/2/16	1/2/16	1/2/16
178	1/2/16	1/2/16	1/2/16	1/2/16
179	1/2/16	1/2/16	1/2/16	1/2/16
180	1/2/16	1/2/16	1/2/16	1/2/16
181	1/2/16	1/2/16	1/2/16	1/2/16
182	1/2/16	1/2/16	1/2/16	1/2/16
183	1/2/16	1/2/16	1/2/16	1/2/16
184	1/2/16	1/2/16	1/2/16	1/2/16
185	1/2/16	1/2/16	1/2/16	1/2/16
186	1/2/16	1/2/16	1/2/16	1/2/16
187	1/2/16	1/2/16	1/2/16	1/2/16
188	1/2/16	1/2/16	1/2/16	1/2/16
189	1/2/16	1/2/16	1/2/16	1/2/16
190	1/2/16	1/2/16	1/2/16	1/2/16
191	1/2/			

# 3. Results

## 3.1 Mandatory information

### 3.1.a Reference report

This Charpy test is conducted adhering to the standards provided in the standard ISO 148-1

### 3.1.b Identification of the test piece (e.g. type of steel and cast number)

This information was not available due to the sample preparation not adhering to the standard as explained in chapter 2.1.

### 3.1.c Size of the test piece, if other than the standard test piece

The measured values before the test were the width and thickness of the test pieces. The width means the distance between the notched face and its opposite face (ISO148). The thickness means the dimension, which is perpendicular to the width and parallel to the notch (ISO 148).

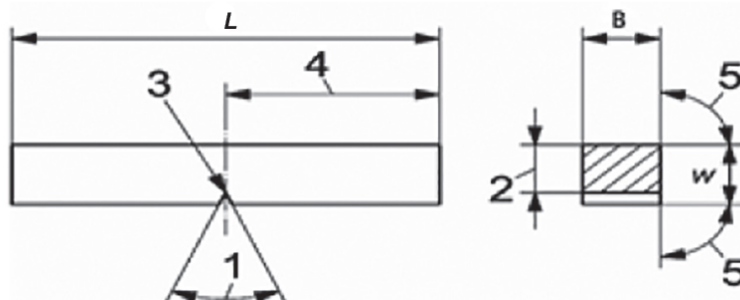


Figure 9. V-notch geometry (ISO 148).

Table 2. Width and length of the test specimens before the test.

Number of specimen	Width before the test (mm)	Thickness before the test (mm)
11	9,90	10,03
12	9,87	10,04
13	9,92	10,00
15	9,92	10,01
16	9,96	10,05
18	9,95	9,98

### **3.1.d Temperature of the test specimens (Table 2)**

The temperatures of the test specimens are shown in the Table 2 below. Specimen 11 was at room temperature before the test. Specimens 12-16 were conditioned in a mixture of liquid nitrogen and ethanol before test test, in which the temperature of -30 celsius was achieved. Specimen 18 was conditioned in pure liquid nitrogen, in which the temperature of -60 celsius was achieved.

### **3.1.e Absorbed energy**

Table 3. Temperature of the test specimens before test and absorbed energy of the test specimens during the test.

Number of specimen	Temperature in °C	Absorbed energy KV2 (J)
11	19,5	161
12	-30 (liquid nitrogen + ethanol)	120
13	-30	64
15	-30	70
16	-30	57
18	Liquid nitrogen (-60)	10

### **3.1.f Whether the specimen, or the majority of specimens in a group of specimens were broken**

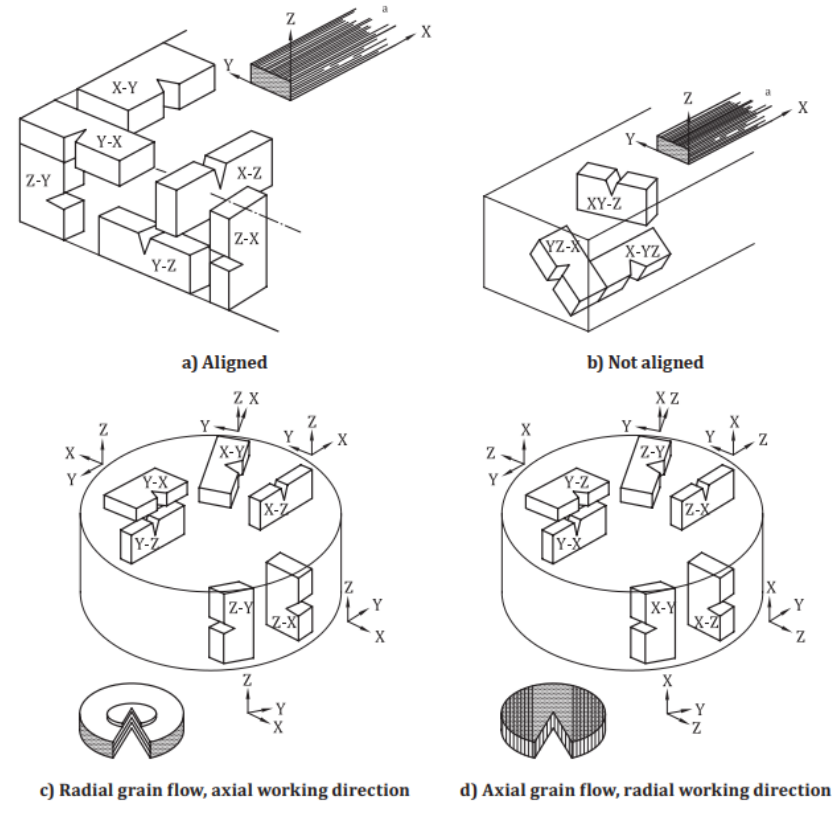
Only specimen 18, which was conditioned in liquid nitrogen, fully broke during the test. All other samples had a small shear lip connecting the two pieces together. However, this is presumed to not affect the test results in a significant way.

### **3.1.g Any abnormalities that could have affected the test**

The test samples 12-18, (conditioned to subzero temperatures), were not moved from the conditioning liquid to the machine quickly enough for the conditioning temperature to remain stable. This introduces some variation in the actual temperatures at which the samples fractured. The position of the test piece in the testing machine can vary a little between the different test samples, since the test sample is put to the machine by the pliers, in which the position of the sample can vary.

## 3.2 Optional information

### 3.2.a Test piece orientation (ISO 3785)



a Grain flow.

Figure 10. Test piece orientation.

This is the figure from ISO 3785 standard, which outlines orientation for notched specimens used for impact testing, such as the Charpy test. Based on the texture of the fracture surface, we determine that the grain orientation of the material is the Aligned type.

### 3.2.b Initial potential energy of the testing machine, in joules

The initial potential energy of this testing machine is 300 Joules, as observed from the below figure



Figure 11. Initial potential energy maximum value  $K_p = 300\text{J}$  as seen inside the red box.

### 3.2.c Lateral expansion (Annex B)

The lateral expansion is the difference of the thickness before and after the Charpy test.

$$\text{Lateral Expansion (mm)} = \text{Thickness after the test (mm)} - \text{Thickness before the test (mm)}$$

In the Charpy impact test, when the notched specimen is struck and fractured, it doesn't just break apart. If the material is ductile, the specimen will also exhibit some degree of deformation, which can be measured as an increase in thickness at the notch. This increase in thickness due to the impact is termed "lateral expansion". For example, this is how we measure the thickness after testing, which is 11.53 mm.



Figure 12. Thickness of the test specimen after testing.

The lateral expansion can be simply calculated from Excel as a new column data. Most of the case, the thickness after the test will be larger, resulting in positive lateral expansion. Since there were lots of Charpy tests, we only showed a subset of measurements in the figure below.

Thickness before the test (mm)	Thickness after the test (mm)	Lateral expansion (mm)
9.89	11.55	1.66
10	11.38	1.38
9.99	11.41	1.42
9.95	11.51	1.56
10.03	11.30	1.27

Figure 13. Lateral expansion calculated from Excel.

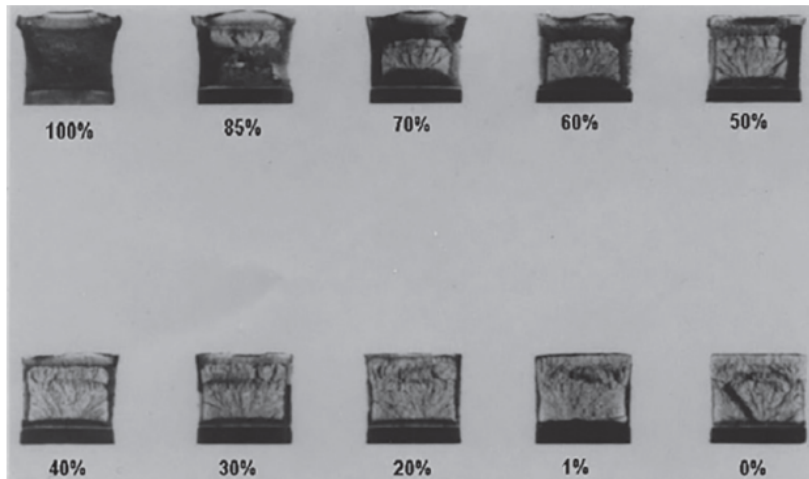
### 3.2.d Shear fracture appearance (Annex C)

These are the fracture surfaces of all specimens recorded in all lab sessions, including the 6 specimens from our group, based on 5 different temperature values.



Figure 14. Fracture surface of all test specimens.

From Annex C, we can derive the percentage of shear fracture based on the fracture surface appearance



a) Fracture appearance charts and per cent shear fracture comparator



b) Guide for estimating fracture appearance

Figure 15. ISO standard estimation for ductile fracture appearance.

The summary table of the behavior on the fracture surface is listed in table 4.

*Table 4. Summary table of behavior on the fracture surface.*

temperature (C)	20	-10	-20	-30	-65
fracture mode	Totally ductile	Mostly ductile, a little brittle around the edge	Half area is ductile and another half is brittle	Mostly brittle, a little ductile around the edge	Totally brittle
shear fracture percentage (%)	80-100%	60-80%	30-60%	10-30%	0-10%

### 3.2.e Absorbed energy/temperature curve (Annex D.1)

The absorbed energy/temperature curve (K/T curve) shows the energy absorbed as a function of the test temperature for a given type of test piece. In general, the curve is obtained by drawing a fitted curve through the individual values. The shape of the curve and the scatter of the test values are dependent on the material, the specimen shape and the impact velocity. In the case of a curve with a ductile-to-brittle transition zone, a distinction is made between the upper-shelf zone, transition zone and the lower-shelf zone. The absorbed energy/temperature curve is obtained using the Curve Fitting toolbox in MATLAB

<https://se.mathworks.com/products/curvefitting.html>

The parametric equation for the curve is the Boltzmann fitting function, whose formula is:

$$y = f(x) = a + \frac{b-a}{1+\exp\left(\frac{c-x}{d}\right)} \quad (1)$$

where a,b,c,d are parameters that need to be fitted. We need to minimize the mean squared error. Initially, we set the range as follows. The starting point is taken from literature.

*Table 5. Fitting parameters and minimizing the mean squared error in matlab.*

Coefficients	StartPoint	Lower	Upper
a	10	-300	300
b	100	-300	300
c	-10	-300	300
d	10	-300	300

Then, MATLAB returns the fitted curve and the optimal values for a,b,c,d as below. This is the absorbed energy/temperature curve required in annex D.1

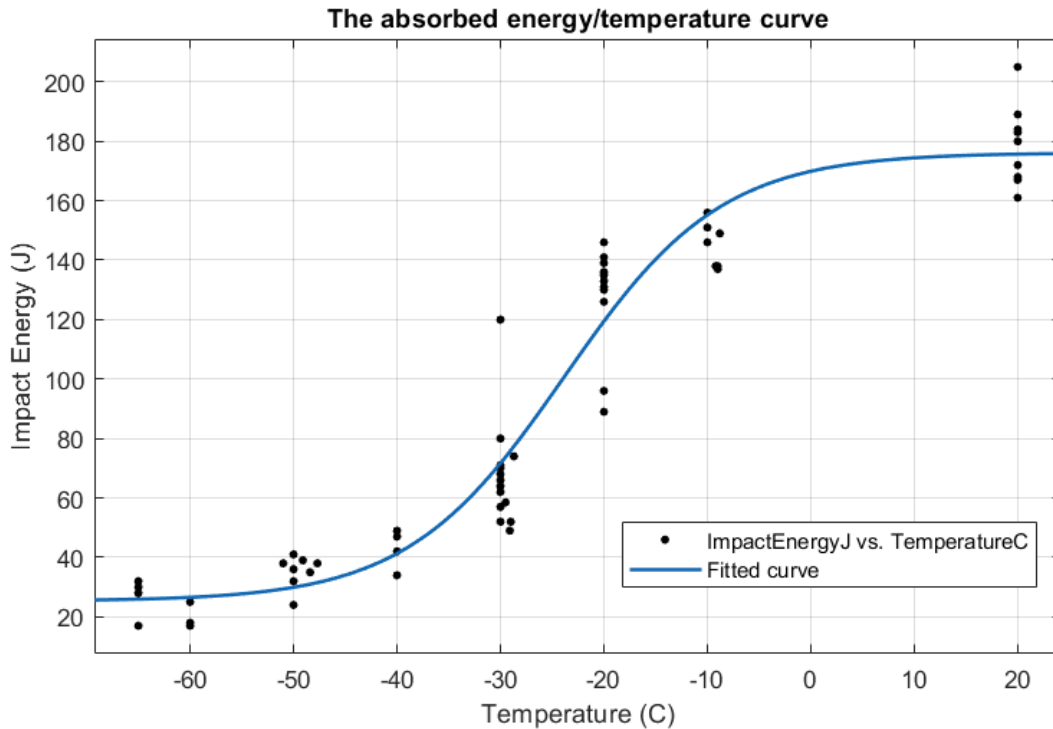


Figure 17. Fitted curve created from the points obtained in Figure 16 with Matlab.

We can measure the quality of this fitting curve by the Sum of Squares errors and R-square. An R square of 0.937 suggests high correlation between the data points and the fitting curve.

Goodness of Fit	
	Value
SSE	1.2989e+04
R-square	0.9370

Figure 18. SSE and R-square obtained with Matlab.

Finally, we obtain the fitting parameter values of  $a, b, c, d$  from the table below:

*Table 6. Fitting parameter values of  $a, b, c, d$*

Coefficients and 95% Confidence Bounds			
	Value	Lower	Upper
<b>a</b>	25.2953	16.7449	33.8457
<b>b</b>	176.1301	166.9880	185.2723
<b>c</b>	-23.8415	-25.7100	-21.9729
<b>d</b>	7.5851	5.8073	9.3629

### 3.2.f Lateral expansion/temperature curve

Using the exact previous procedure, we obtain the lateral expansion/temperature curve required in annex D.1

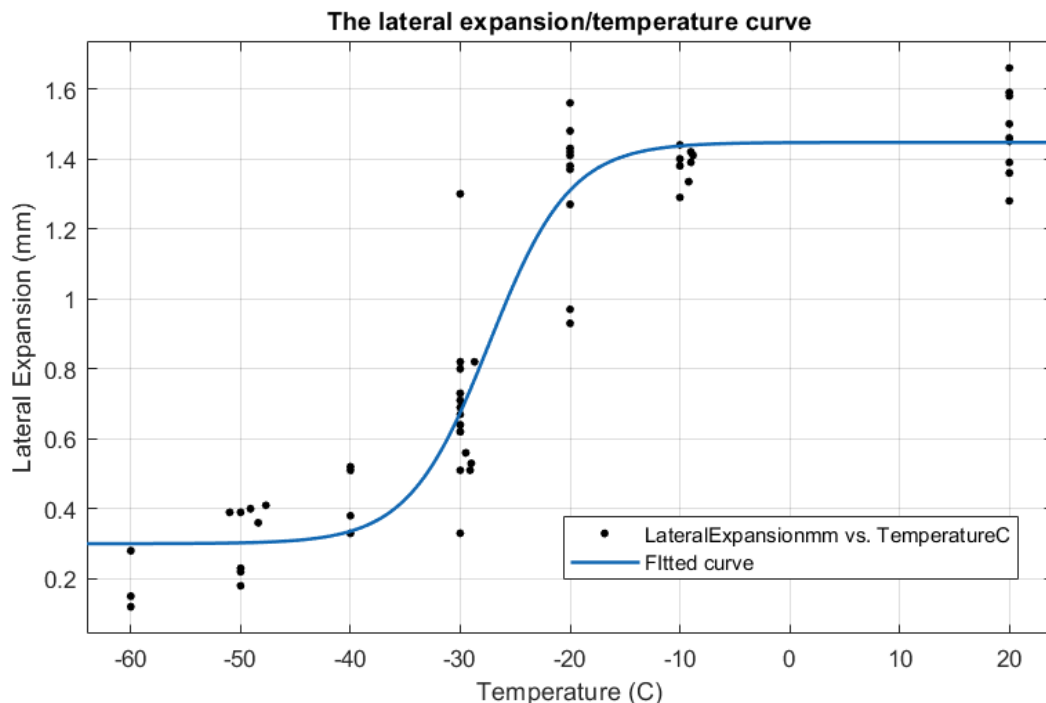


*Figure 19. Lateral expansion/temperature curve.*

Fitting parameter values of a,b,c,d:

*Table 7. Fitting parameter values of a,b,c,d*

Coefficients and 95% Confidence Bounds			
	Value	Lower	Upper
a	0.3002	0.2138	0.3866
b	1.4472	1.3638	1.5305
c	-27.3487	-28.9066	-25.7908
d	3.6759	2.2772	5.0746

*Table 8. Fitting curve quality*

Goodness of Fit	
	Value
SSE	1.4971
R-square	0.8986

### 3.2.g Shear fracture appearance/temperature curve

Using the exact previous procedure, we obtain the shear fracture appearance/temperature curve required in annex D.1

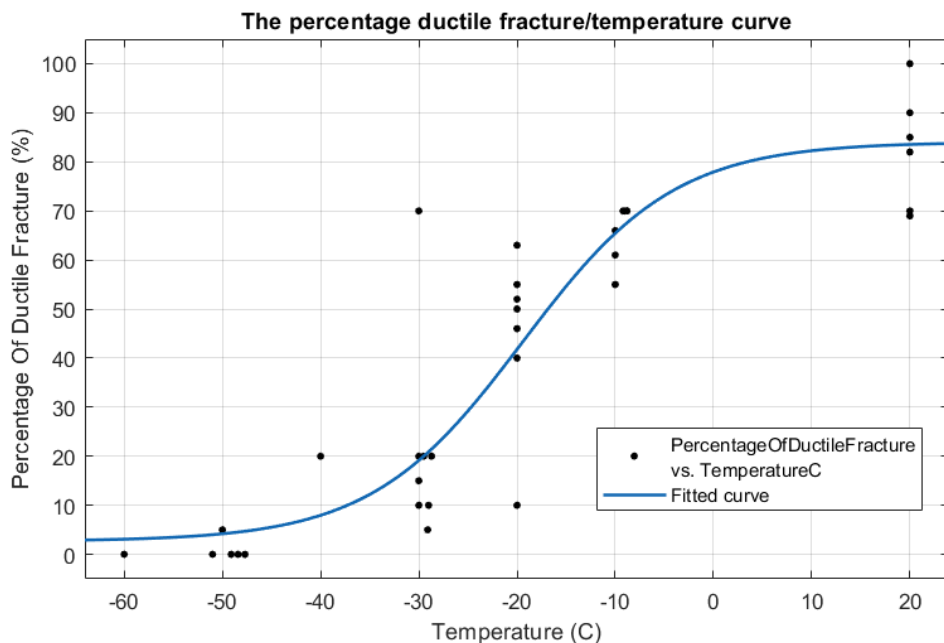


Figure 20. Shear fracture appearance/temperature.

Table 9. Fitting parameter values of  $a, b, c, d$

Coefficients and 95% Confidence Bounds			
	Value	Lower	Upper
<b>a</b>	2.6602	-5.0304	10.3508
<b>b</b>	84.0315	75.6913	92.3718
<b>c</b>	-19.4031	-22.5555	-16.2506
<b>d</b>	7.7304	4.8351	10.6258

Table 10. Fitting curve quality

Goodness of Fit	
	Value
SSE	8.0471e+03
R-square	0.8563

### 3.2.h Transition temperatures and determination criteria (Annex D.2)

The transition temperature is the temperature at which a material transitions from a brittle fracture mode to a ductile fracture mode. This transition is typically characterized by a significant change in the amount of energy absorbed during the test, as well as changes in the fracture appearance. From the ISO 148-1 report, annex D.2, it says that the transition temperature,  $T_t$ , characterizes the position of the steep rise in the absorbed energy/temperature curve. Since the steep rise usually extends over a fairly wide temperature range, there can be no generally applicable definition of the transition temperature. The following criteria are however used for determining the transition temperature:

- a)  $T_{t27}$ , corresponding to a specific value of absorbed energy, e.g. KV8 = 27J;

Since it is apparent that 27J is not lying in the transition region, we can use another energy level to determine the transition temperature. One of them is 60J, which is used in this report.

<https://op.europa.eu/en/publication-detail/-/publication/e40b0ee0-0fe8-473e-bc3c-2372ad19e504/language-en>

The inverse of the Boltzmann function is:

$$Temp = c - d \ln\left(\frac{b-a}{Energy-a} - 1\right) \quad (2)$$

Plugging in these values:

Coefficients and 95% Confidence Bounds				
	Value	Lower	Upper	
a	25.2953	16.7449	33.8457	
b	176.1301	166.9880	185.2723	
c	-23.8415	-25.7100	-21.9729	
d	7.5851	5.8073	9.3629	

$a = 25.2953$ ,  $b = 176.13$ ,  $c = -23.8415$ ,  $d = 7.5851$ , Energy = 60J, we have the transition temperature as:

$$T_{t60} = -33.0 \text{ C (Answer)}$$

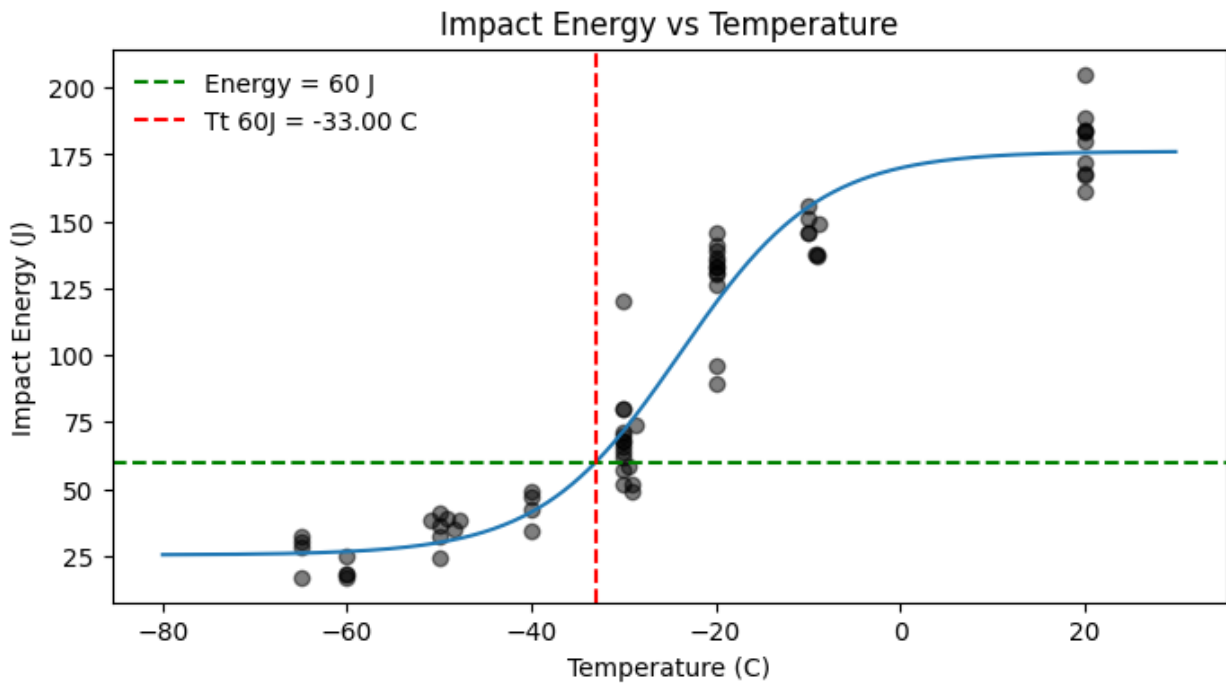


Figure 21. Impact energy vs temperature.

b)  $T_{t50\%us}$ , corresponding to a percentage of the absorbed energy of the 50% upper-shelf value,

The energy absorbed by a specimen during fracture is plotted against temperature, resulting in a characteristic "S" shaped curve. This curve can be divided into three distinct regions: the lower shelf, the transition region, and the upper shelf. The energy absorbed in the upper shelf is relatively high and consistent, with little variation with temperature.

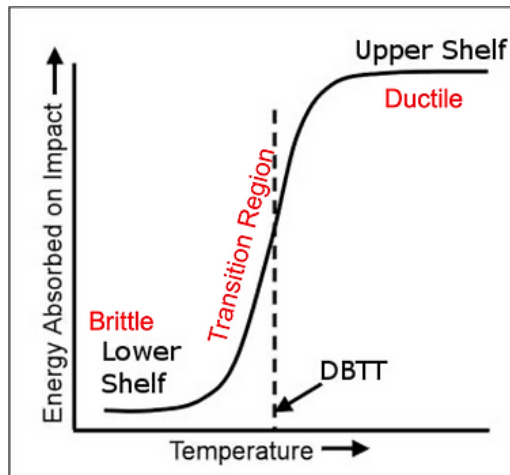
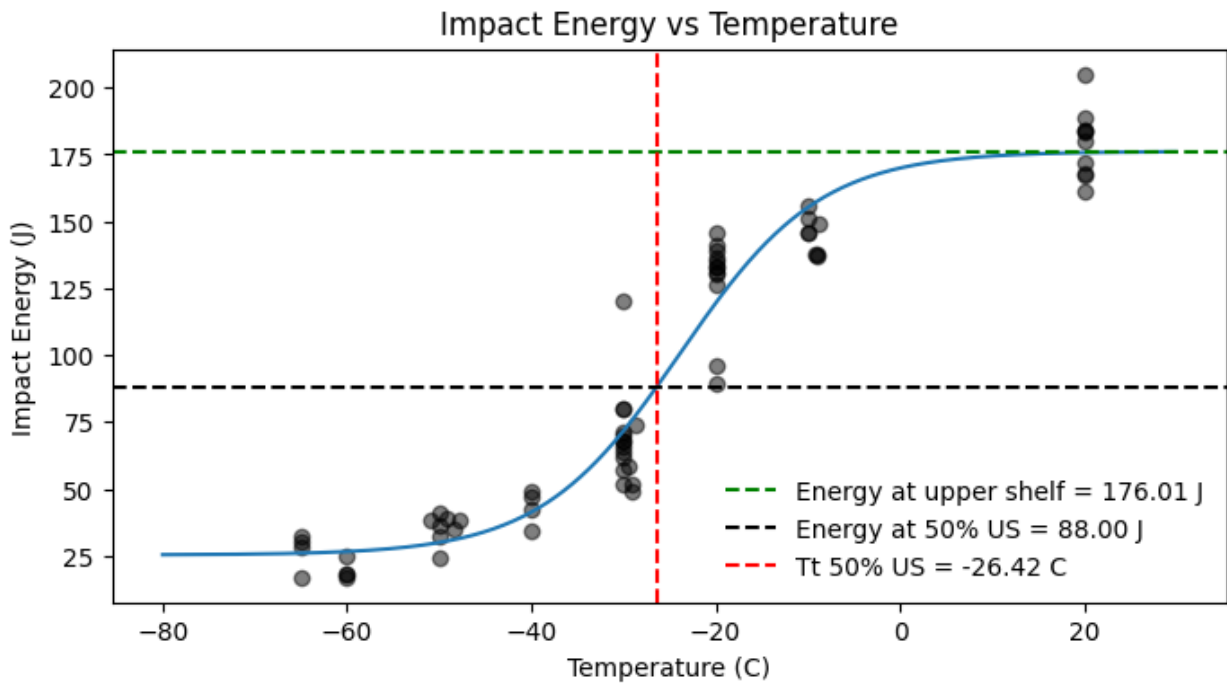


Figure 22. Transition temperature curve.

In this method, the transition temperature is determined at the level of half of the upper shelf. The answer is  $T_{t50\%us} = -26.42$  C, using the inverse Boltzmann function like the above analysis.



*Figure 23. Impact energy vs temperature curve.*

c)  $T_{t50\%SFA}$ , corresponding to a particular proportion of shear fracture, e.g. 50 %;

The percentage of the ductile fracture column can be derived from the image of the fracture surface and refer it back to the manual page 22. The proportion of shear fracture is essentially referring to the percentage of the fracture surface that exhibits ductile characteristics, which corresponds to the column Percentage of ductile fracture (%). The temperature at which the fracture surface is 50% shear (or ductile) and 50% brittle is identified as  $T_{t50\%SFA}$ . This temperature is significant because it represents a point within the transition region between the material's brittle and ductile behavior. The answer is  $T_{t50\%US} = -16.85$  C, using the inverse Boltzmann function like the above analysis.

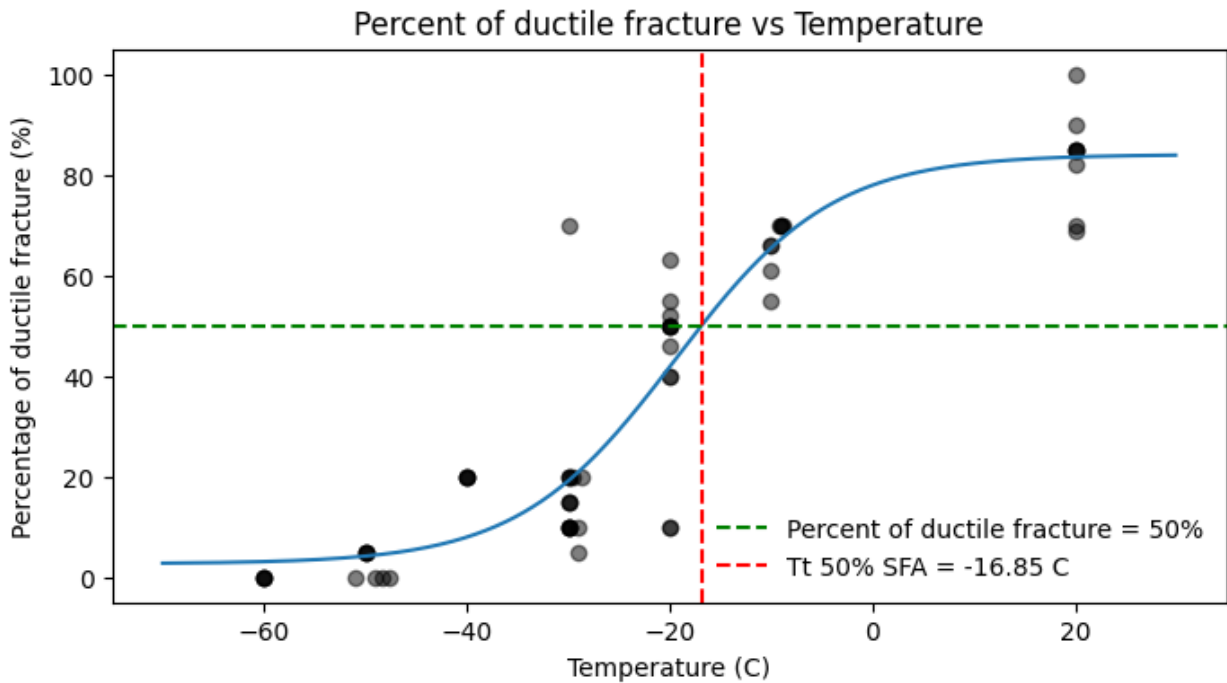


Figure 24. Percentage of ductile fracture and temperature plotted in transition temperature curve.

d)  $T_{t0,9}$ , corresponding to a particular amount of lateral expansion, e.g. 0.9 mm.

Lateral expansion is a measure of the ductility of the material during the test. A higher lateral expansion indicates more ductile behavior, while a lower value suggests more brittle behavior. This temperature provides a quantitative measure of the material's ductile-to-brittle transition based on a specific ductility criterion (0.9 mm of lateral expansion in this case). The answer is  $T_{t0,9} = -16.85 \text{ C}$ , using the inverse Boltzmann function like the above analysis.

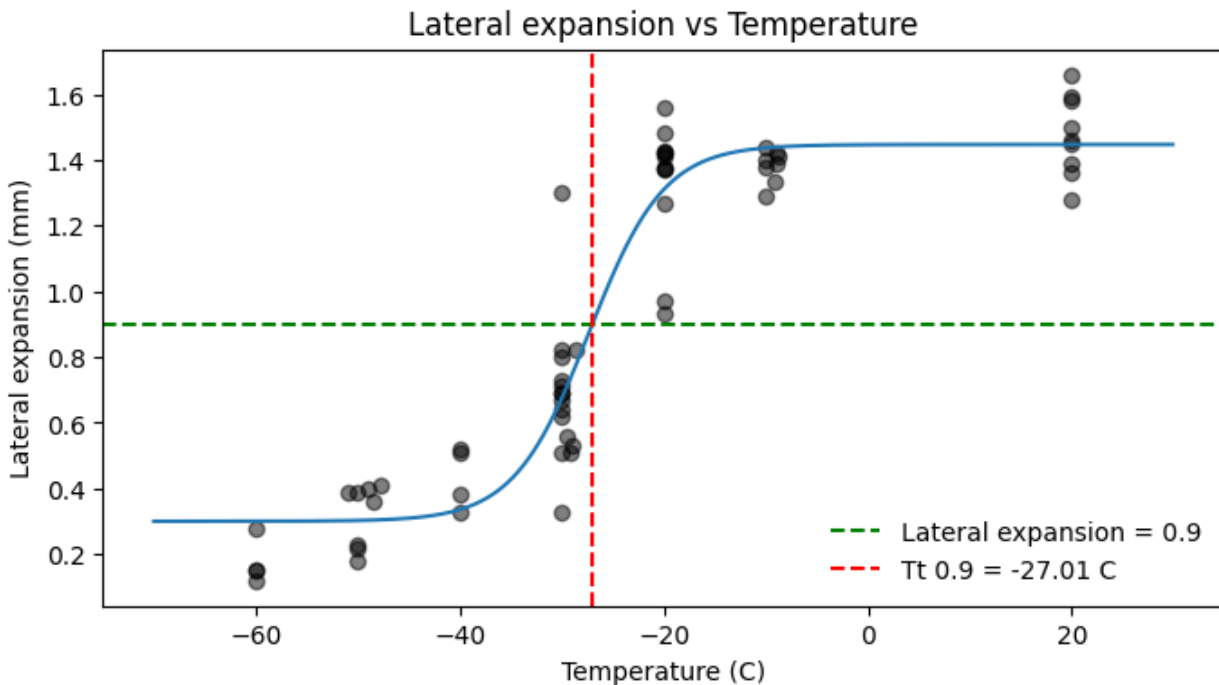


Figure 25. Lateral expansion and temperature plotted in transition temperature curve.

To sum up, the transition temperature according to the four methods from annex D.2 are:

Table 11. Final results for transition temperature using the different methods.

T <sub>t</sub> 60J	T <sub>t</sub> 50% US	T <sub>t</sub> 50% SFA	T <sub>t</sub> 0,9
-33.0 C	-26.42 C	-16.85 C	-27.01 C

Two methods result in nearly similar temperatures, which are T<sub>t</sub> 50% US and T<sub>t</sub> 0,9. Therefore, we believe that the transition temperature is around -26.7 C.

### 3.2.i Number of test pieces which were not completely broken in the test

We have tested 6 samples and none of them were completely broken into two halves in the test.

### 3.2.j Date of the most recent full direct and indirect verifications

Date of full direct verification: 10th September 2023 (Laboratory experiment)

Date of indirect verification: 21th September 2023 (Standard report and Literature review)

### 3.2.k Measurement uncertainty of the absorbed energy (Annex E)

- First step, the mean observed KV value,  $x_{\text{mean}}$ , is calculated, as well as the standard uncertainty,  $u(x_{\text{mean}})$ , which is calculated using Formula (E.3). We only calculate for 20 C samples, since the same procedure can be applied for all temperatures.

Sample's absorbed energy measurements at 20 C: [183. 184. 161. 189. 167. 180. 184. 205. 168. 172.]

Number of samples n: 10

Mean KV,  $x_{\text{mean}}$ : 179.3 J

Standard deviation of n = 10,  $s_x$ : 12.82

Standard uncertainty of the mean observed KV,  $u(x_{\text{mean}})$  calculated according to Formula (E.3)

$u(x_{\text{mean}}) = 4.055$

- In the second step, the raw results (without correction for bias) were combined with the results of the most recent indirect verification test, for which reference test pieces of different energy levels were used. Because there is no machine bias (adhering to the ISO 148-2 standard), we have  $B_V = 0$ . Also, there is no temperature standard, so  $T_x = 0$ . Based on Formula E.1, we have  $KV_{\text{mean}} = x_{\text{mean}} = 179.3 \text{ J}$  for samples in 20 C, and its uncertainty is around 4 J

## 4. Discussion

### 4.1 Result analysis

Impact toughness is a measure of a material's ability to absorb energy during plastic deformation. It is expressed in terms of energy per unit cross section area. Therefore, the impact toughness for each specimen of a certain temperature is calculated as

Impact Toughness ( $\text{J/mm}^2$ ) = Impact energy (J)/(Specimen cross section area ( $\text{mm}^2$ ))

with Specimen cross section area ( $\text{mm}^2$ ) = Width before the test (mm)  $\times$  Thickness before the test (mm)

In Excel, this can be simply calculated using those four columns. Impact toughness looks like below

Impact Energy (J)	Impact toughness ( $\text{J/mm}^2$ )	Width before the test (mm)	Thickness before the test (mm)
183	1.82	10.15	9.89
136	1.36	10.01	10
126	1.26	10.04	9.99
146	1.46	10.05	9.95
130	1.29	10.02	10.03

## 4.2 Differences in fracture behavior in various temperatures

Some metals, particularly ones with BCC structure, are susceptible to low-temperature embrittlement (Chernov et al. 2016), a phenomenon where the fracture mechanisms transition from ductile to brittle over a relatively narrow temperature range. Therefore, most structural steels, which have high ferrite content, are affected by this phenomenon. The susceptibility of BCC packed metals is related to their low dislocation mobility in low temperatures, which limits the material's ability for plastic deformation, preventing ductile tearing and initiating a brittle fracture. Practically all BCC metals have odd axes of symmetry for slipping in the crystal plane  $<111>$ , which leads to high Peiers barrier, inhibiting dislocation movement (Chernov et al., 2016).

As mentioned, the transition between ductile and brittle fractures modes does not occur in a specific temperature, but gradually across a temperature range. As ductile fracture absorbs a high amount of energy, whereas brittle fracture absorbs very little energy, the gradual change between the two fracture modes leads to different absorbed energy values being measured in test series conducted in different temperatures.

The gradual transition is visible in the fracture surfaces depicted in figure 14. Samples fractured in room temperature have a high percentage of ductile fracture, which is visible as large shear lips and relatively flat surface with matte appearance surrounding a small rough, but shiny area. The matte surface is produced by ductile tearing, and it is rather flat on a macroscopic scale, as the direction of crack propagation follows the highest mode I loading. The material plastically deforms to accommodate this. On a microscopic level, however, high plastic deformation leads to a very rough, "dimpled" surface that reflects light poorly, which produces the matte appearance. The center area is produced by brittle fracture, during which there is negligible plastic deformation ahead of the crack tip. Therefore, the crack has to constantly change direction to propagate along slip planes in the crystallographic structure of the material, leaving a surface that appears relatively rough on a macroscopic scale. Under microscopic examination, the brittle area would appear very flat, thus reflecting light well, which results in the shiny, or sparkling, appearance of a brittle fracture surface.

## 4.3 Reliability of results

The Charpy test is standardized, meaning that when performed according to standards ISO 148-1 and 148-2, it can provide consistent results. While the Charpy test provides information about a material's toughness, it is a qualitative rather than a quantitative measure of fracture toughness. It gives an indication of the relative toughness of materials and their behavior over a temperature range but doesn't provide an absolute measure of fracture toughness. The conclusion is that the data is not entirely reliable due to varying measurements, but provides enough information to obtain certain properties such as the transition curves and transitioning temperature.

For example, the specimens at 20 C show a range of different impact energy, with standard uncertainty of 4J. This is because material properties vary due to many factors like microstructure, and processing. Therefore, even samples from the same metal sheet can show some variability in Charpy test results.

To achieve a high level of confidence in the results, multiple samples are typically tested. The exact number can vary based on standards, but a common practice is to test at least **three** samples at each temperature to know for sure their standard deviation. In this lab result, we have around 6 tests for each temperature, which is adequate to determine the impact energy and build the transition curve.

#### 4.4 Brief conclusion

This laboratory exercise has taught students the skills to:

- Read standard manuals in mechanical testing, such as ISO 148-1, 148-2 and 3785.
- Gather testing data to construct transition curves (energy/percentage of shear fracture/lateral expansion v.s temperature) and apply standard methods to find the transition temperatures.
- Calculate uncertainty in result measurements and testing instruments.

This report summarizes the knowledge the students have gained, and it can be used as a reference so others can replicate similar experiments in the future.

## References

Chernov, Vyacheslav & Kardashev, B.K. & Moroz, K.A.. (2016). *Low-temperature embrittlement and fracture of metals with different crystal lattices – Dislocation mechanisms*. Nuclear Materials and Energy. 9. DOI: 10.1016/j.nme.2016.02.002

Hertzberg, R. W. (2012). *Deformation and fracture mechanics of engineering materials*. Wiley.  
<https://ebookcentral-proquest-com.libproxy.aalto.fi/lib/aalto-ebooks/detail.action?docID=2064702#>

Finnish Standards Association SFS. (2016). *Metallic materials. Charpy pendulum impact test. Part 1: Test method (ISO 148-1:2016)*.

Finnish standards Association SFS. (2016). *Metallic materials. Charpy pendulum impact test. Part 2: Verification of testing machines (ISO 148-2:2016)*.